July 2019

Assessment of Excess Thyroid Cancer Risk Following a Hypothetical Radiological Incident in Louisiana and Best-Case Risk Reduction Achieved by Thyroid Blockade

Garrett A. Otis
Louisiana State University and Agricultural and Mechanical College

ASSESSMENT OF EXCESS THYROID CANCER RISK FOLLOWING A HYPOTHETICAL RADIOLOGICAL INCIDENT IN LOUISIANA AND BEST-CASE RISK REDUCTION ACHIEVED BY THYROID BLOCKADE

A Thesis

Submitted to the Graduate Faculty of the
Louisiana State University and
Agricultural and Mechanical College
in partial fulfillment of the
requirements for the degree of
Master of Science

in

The Department of Physics and Astronomy

by
Garrett Otis
B.S., Louisiana State University, 2015
August 2019

Acknowledgements

Foremost, I thank my friend Dr. Charles Wilson and my graduate advisor Dr. Wei-Hsung Wang for introducing me to the field of Health Physics several years ago; without them, I would not have written this thesis. Additionally, ever since I've been enrolled in Louisiana State University's Medical Physics and Health Physics program, Dr. Kenneth Matthews has consistently proven to be approachable and respectful to prospective and enrolled students.

Second, I thank my committee, consisting of Dr. Wei-Hsung Wang, Dr. Kenneth Matthews, and Dr. Jeffrey Blackmon, for their feedback on my thesis. The iterative process of refinement through review and discussion is what creates quality work, and I appreciate their contribution to that process.

Third, I thank those who were not on my committee, yet still provided their insight on matters regarding my thesis when I sought them out. In particular, I thank Dr. Wayne Newhauser, Dr. Charles Wilson, Mr. Amin Hamideh, Mr. Jabari Robinson, and my peers in the Medical Physics and Health Physics program.

Lastly, I thank my family for being emotionally supportive of my decision to return to school and change my career path. I also thank them for their desire to always want what's best for my well-being, because otherwise I would not be where I am.

This work was supported in part by a graduate fellowship from the Nuclear Regulatory Commission.

Table of Contents

Abstract

Radioactive isotopes of iodine are produced by nuclear power plants as a byproduct of nuclear fission reactions. If these isotopes are released into the environment, such as during a breach of containment, they constitute a health risk to exposed individuals. To mitigate the risk of thyroid cancer due to exposure to radioactive iodine, “iodide prophylaxis,” also known as “thyroid blockade,” can be used, usually by administration of potassium iodide (KI). In some areas of the world, KI has been provided to the general public by their governments as a precautionary measure against potential nuclear power plant incidents. However, in the state of Louisiana, only evacuation and sheltering of the general public are the planned response to such incidents. The question of whether Louisiana’s government should provide KI to the public is a question of risk management. This project’s risk assessment provides a framework for determining radiation risk from radioiodine release from a nuclear power plant, enabling an assessment of the potential benefit of providing KI to the general public in Louisiana. In this assessment, a hypothetical radiological incident of similar severity to the Fukushima accident was modeled for a nuclear power plant in Louisiana. Environmental transport of discharged radioactive iodine was modeled with a Gaussian plume model. Thyroid dose was calculated using representative parameters from International Commission on Radiological Protection Publication 71. Age- and sex-specific values of excess relative risk, lifetime attributable risk, and excess lifetime thyroid cancers were calculated. Lastly, the number of excess lifetime thyroid cancers mitigated by thyroid blockade was estimated through two separate approaches. This assessment found that a plume traveling over highly populated parishes near the power plant could result in

approximately 200 excess lifetime thyroid cancers over all age groups. The largest number would likely occur in females exposed as children. Thyroid blockade could potentially mitigate 80 or more of the excess cancers. These results suggest that more comprehensive assessments of KI distribution in Louisiana may be warranted.

Chapter 1. Introduction

1.1. Motivation and Scope

Louisiana's Peacetime Radiological Response Plan (Louisiana Department of Health 2016) states that "During an accident at a fixed nuclear facility, the State of Louisiana will consider recommending the use of thyroid protective drug potassium iodide (KI) within the affected area for emergency workers, and also for institutionalized persons who are unable to evacuate quickly." Providing the thyroid-protective drug KI to the general public as a whole, rather than to only institutionalized persons, is not within the scope of the policy, either before or after such an accident. Rather, sheltering-in-place and evacuation are considered or recommended based upon the anticipated total effective dose equivalent or thyroid committed dose equivalent to affected members of the general public. However, governments in other areas of the world have recently distributed, or expressed an interest in distributing, KI pills to their general public as a precautionary measure against nuclear power plant accidents. For example, Luxembourg undertook a preventive KI distribution campaign in 2014 which made KI pills freely available to all of its inhabitants (Luxembourg 2014). Similar campaigns were conducted in Switzerland in 2014 (Switzerland 2014), Netherlands in 2017 (Netherlands 2017), and Belgium in 2018 (Belgium 2018). Given this trend of governments providing KI pills to their citizens as a precautionary measure against nuclear power plant accidents, should Louisiana consider doing so as well?

The decision for Louisiana to provide KI pills to its general public depends on several factors. These factors include financial cost; benefit regarding thyroid cancer risk mitigation; logistics of storage, distribution, and re-stocking of KI pills; legal issues of

widespread administration; and psychosocial ramifications of implementing such a policy. The purpose of this thesis was to provide a conservative estimation of thyroid cancer risk mitigation provided by KI prophylaxis, which is only one of the factors in determining whether KI pills should be provided to Louisiana's general public.

The first goal of this assessment was to model a hypothetical worst-case exposure scenario due to an unintended discharge at a nuclear facility in Louisiana, and thereby estimate the excess thyroid cancer risk posed to the general public as a result of the incident. The second goal is to estimate the potential thyroid cancer risk reduction provided by KI prophylaxis, assuming the general public has prompt access to KI pills.

Chapter 2, "Background and Review," provides a review of relevant terminology and concepts that are necessary to interpreting the results of this assessment. Chapter 2 also provides a detailed discussion of radioactive iodine, with an overarching emphasis on toxicological effects as a result of exposure. Chapter 3, "Methods and Materials," details how this assessment was performed and includes justifications of the assumptions and quantitative values that were used in calculations. Chapter 4, "Results and Discussion," presents plots and tables representing the results, interpretation of the results and their implications, a discussion of the limitations associated with this assessment, suggestions for future work, and lastly, the assessment's conclusions.

Chapter 2. Background and Review

2.1. Dimensions of Risk

For radiological risk assessment, risk is a function of source terms, environmental transport, exposure factors, conversion to dose, and conversion of dose to risk (Till 2008). The “source term” is the quantity of radioactive material released into the environment. The source term is used to derive radionuclide concentrations at locations other than the source’s location. In cases of retrospective analysis of a radiological incident, such as an unintended discharge from a nuclear plant, downwind monitoring stations and field measurements are used to estimate the source term. A hypothetical incident was considered for this assessment, so estimates of a plausible source term were derived from historical accidents (see Chapter 3).

“Environmental transport” refers to the dispersion of radionuclides into the environment after emission from the source. Environmental transport models are specific to the scale of analysis; for example, macroscale atmospheric modeling involves transport over several thousand kilometers and considers weather fronts, pressure gradients, and rotation of the earth in addition to other large-scale factors. Mesoscale and microscale atmospheric modeling consider more granular factors, such as convective activity of the Earth’s surface (for mesoscale; ~100 km transport), or surface roughness and building wake (for microscale; <~1 km transport).

“Exposure factors” refer to parameters of the exposed population that are necessary to calculate dose and risk. Examples of exposure factors are breathing rate, time spent outdoors per day or week, and consumption of particular foods. The exposure factors

should be as representative of the exposed individuals as possible to minimize uncertainties in dose and risk calculations.

"Conversion to dose" involves calculating radiation dose from either external exposure or intake of radionuclides. For example, dose coefficients from the International Commission on Radiological Protection (ICRP) allow calculation of committed effective or equivalent dose for a given amount of intake. (The ICRP is a non-governmental organization that develops recommendations for government agencies regarding radiological protection.) The dose coefficients depend upon the pathway of intake and the form of the radionuclide. Generally, such coefficients have a large amount of uncertainty due to variability of relevant biological factors among individuals in a population.

"Conversion of dose to risk" involves converting calculated dose into an estimate of risk for a chosen endpoint. For this assessment, the calculated risk pertained to radiation-induced cancer. Using data from atomic bomb survivors, atomic weapons testing, nuclear power plant accidents, and nuclear medicine, the Biological Effects of Ionizing Radiation (BEIR) committee has developed risk models for radiation-induced cancers (National Research Council 2006). The BEIR committee's cancer risk models are chiefly dependent upon dose, sex, age at exposure, time since exposure, and age at risk determination (attained age). The cancer risk models are also dependent upon the type of cancer. This assessment used the model for thyroid cancer (see Section 2.2).

2.2. Communication of Risk

For reporting the results of this assessment, several different metrics are used to communicate risk. Absolute risk (AR) describes the rate of disease in a population.

Relative risk (RR) is a ratio of two rates of disease (two ARs) in a population, where the two rates differentiate between an exposed group (AR_e) and a non-exposed or reference group (AR_n). Mathematically, RR = AR_e/AR_n.

Excess relative risk (ERR) is the fractional increase of the exposed group's rate of disease when compared to the reference group; alternatively, if multiplied by 100, the ERR is the percentage increase over the reference group's rate of disease. Mathematically, ERR = RR – 1 if not expressed as a percentage. If the ERR is greater than zero, then the exposed group has an elevated risk.

The thyroid cancer risk model used in this assessment was from the BEIR VII report, wherein the committee developed a preferred model based upon a pooled analysis of seven studies that investigated the excess risk of thyroid cancer as a function of absorbed dose (National Research Council 2006). The thyroid cancer model takes the form of:

$$ERR(D, e) = \beta * D * \exp[-0.83(e - 30)] \quad [1]$$

where ERR is the excess relative risk, D is the absorbed thyroid dose in Gy, β is a unitless sex-specific parameter, and e is the age at exposure in years. The sex-specific parameter for males is β_M = 0.53, with a 95% confidence interval of 0.14 to 2.0. For females, the parameter is β_F = 1.05 with a 95% confidence interval of 0.28 to 3.9.

Excess absolute risk (EAR) describes the above-baseline or above-reference rate of disease in a population; mathematically, it is the algebraic difference between two ARs. If the EAR is greater than zero, then it implies disease occurring at a rate above the natural incidence. EAR can be calculated using ERR if the ERR is multiplied by the baseline cancer-specific incidence or mortality rate. Lifetime Attributable Risk (LAR) represents

the risk of cancer incidence or mortality over a lifetime. LAR is a summation of EAR over a lifetime, with each term of the sum weighted by the probability of surviving to subsequent ages up to a specified age. Calculation of LAR depends on several variables, and the values used in its equation depend on available data, so detailed discussion of the LAR calculation is deferred to Section 3.4.

2.3. Radioactive Iodine

2.3.1. Synthesis

Of all isotopes of iodine, only ^{127}I is stable; all others are radioactive (referred to as radioiodines). Radioiodines occur in nature in only trace amounts formed by cosmic bombardment (Knolls Atomic Power Lab 2010). One additional natural source of radioiodines is the exceptionally rare event of a naturally occurring self-sustaining uranium fission reactor, such as the Oklo reactor in Africa over one billion years ago, which produces radioiodines as fission products (Gauthier-Lafaye 1996).

The presence of substantial amounts of radioiodines on Earth are due to man-made synthesis, such as in atomic weapons testing, nuclear power plant accidents, and fuel reprocessing (Prăvălie 2014, Hou 2003). Of the radioiodines produced by such reactions, the most relevant isotope regarding toxic effects in humans is ^{131}I due to its high uranium fission yield of 2.89% and half-life of 8.023 days (Knolls Atomic Power Lab 2010). The high fission yield of ^{131}I allows it to be produced in large quantities per kilowatt of thermal energy produced, and its half-life is long enough for it to be dispersed into the environment. Such characteristics of ^{131}I make it a consistent threat after nuclear power plant incidents involving a breach of containment.

2.3.2. Exposure to Humans, Flora, and Fauna

There are many different pathways for exposure to radioiodoines. Radioiodine can exist as a particulate, a vapor, or as a solution with the iodine dissolved in water. Radioiodines can pose an external threat and/or an internal threat depending on concentration of, distance from, time spent near, and shielding around the source. For the Chernobyl accident which occurred in 1986, the prominent pathway through which the general public was exposed to ^{131}I and other radioiodines was by ingestion of contaminated food and drink (mostly milk) (Higley 2006). However, in the modern United States the most likely pathway for exposure to radioiodines immediately after a nuclear incident is inhalation of a radioiodine-containing plume rather than ingestion of contaminated food and drink; this is due to food testing and interdiction procedures that would halt the distribution of contaminated food and drink in the event of such an incident. Such limits are discussed in Section 2.3.3.

Non-human animals can be exposed to radioiodines through the same pathways as humans, although they are more susceptible to intake by ingestion due to an inability to prevent them from ingesting contaminated food or drink after deposition of radioiodine onto vegetation or bodies of water in affected areas. Additionally, at sufficient concentrations, radioiodines can pose a threat to flora if deposited onto soil near plants or onto trees. Because the emissions of radioiodines includes gamma rays and beta particles, they present an external hazard to the flora upon which they are deposited. For example, in the exclusion zone of Chernobyl where large amounts of radioactive cesium and iodine were deposited, coniferous trees were killed and deciduous trees suffered partial damage as a result of acute external irradiation (Alexakhin 1994).

2.3.3. Exposure Limits

Because ^{131}I and other radioiodines are radioactive, they can contribute to an exposed individual's cumulative radiation dose over a period of time. Methodologies have been developed to approximate an acceptable limit of exposure based upon a radionuclide's properties and route of exposure.

The derived air concentration (DAC) is used to approximate a limit on the average air concentration of a specific radionuclide (ICRP 2015). The DAC depends on an assumed breathing rate, number of working hours in a year, dose coefficient representing either committed effective dose per unit intake or effective dose due to submersion in a radioactive cloud, and some annual effective dose limit. The DAC separately considers internal radiation dose from inhalation vs. external dose from submersion within a radioactive cloud. The Nuclear Regulatory Commission (NRC) imposes a limit for inhalation DAC of 740 Bq/m^3 for ^{131}I (CFR 2019). Such limits are radionuclide-specific.

The Safe Drinking Water Act, imposes an effective dose limit due to beta particles and gamma photon emission (which therefore includes any radioiodines) present in drinking water at 4 mrem/year (CFR 2002). Assuming no other man-made radionuclides present, an ingestion of 2 liters of drinking water per day for 365 days, and an ingestion dose coefficient of 2.2 μrem/Bq for ^{131}I (ICRP 2012), that dose limit translates to a concentration limit or Maximum Contaminant Level (MCL) of 2.5 Bq/L.

The Food and Drug Administration (FDA) provides recommendations called Derived Intervention Levels (DILs) which are based upon the consumption of radionuclide-contaminated food that, without intervention, would potentially lead to a committed

effective dose established by a Protective Action Guideline (PAG) (FDA 2005). A PAG is a projected dose to an individual from a release of radioactive material at which a specific protective action to reduce or avoid that dose is recommended (EPA 2017). For ^{131}I, the FDA recommends a DIL of 170 Bq per kg of a diet. Like other limits, this is radionuclide-specific.

A Derived Response Level (DRL) is a level of radioactivity in an environmental medium that would be expected to produce a dose equal to its corresponding PAG (EPA 2017). The DRL's intended use is to provide a recommendation for making quick decisions during time-critical scenarios involving accidental radiological releases (EPA 2017). As a "default" DRL for various radionuclides in drinking water, the EPA recommends that radionuclide levels are assumed to be constant (i.e. replenished) to provide greater assurance of conservatism. Assuming one year of constant exposure, the DRL for ^{131}I in drinking water corresponds to 820 pCi/L for pregnant women, nursing women, and children of age 15 and younger (100 mrem PAG). For the general population (500 mrem PAG), the DRL for ^{131}I in drinking water is 10,000 pCi/L.

2.3.4. Biotransformation and Toxic Effects

Radioactive iodine and stable iodine are metabolized identically. Upon intake by humans, dietary iodide is absorbed through the small intestine, transported into blood, and either absorbed by the thyroid gland to be used in the synthesis of thyroid hormones or excreted through urine (Leggett 2017). With the iodide in blood, a thyroid follicular cell (thyrocyte) uses a sodium-iodide symporter to actively transport the iodide into the cell. Once inside the cell, the iodide is moved into the colloid (viscous fluid in the central cavity of a thyroid follicle) via the anion transport protein pendrin. In the colloid, thyroid

peroxidase (TPO) performs several critical steps in the creation of thyroid hormones (Ruf 2006). TPO oxidizes the absorbed iodide and adds the oxidized iodide to the amino acid tyrosine to create monotyrosine (MIT) and diiodotyrosine (DIT). TPO either couples MIT and DIT to create the thyroid hormone triiodothyronine (T3), or couples two DIT to create the thyroid hormone thyroxine (T4). T3 is also produced from T4 via 5'-deiodinase in peripheral tissues, which is the more prominent mode of T3 synthesis (Kimura 1987).

The hormones T3 and T4 are released into circulation and subsequently bind to nuclear receptors at various peripheral tissue cells, which lead to increases in metabolism and protein synthesis. As a consequence, if radioactive iodine is absorbed instead of stable iodine, the thyroid gland and the peripheral tissues where T3 and T4 are circulated are subject to beta particle and gamma radiation. Due to the thyroid gland's very slow transference of organic iodine (as T3 and T4) to blood relative to other organs (Leggett 2017), the thyroid gland is the target tissue that receives the most dose from accumulation of radioiodine. The most substantial toxic effect as a result of inhalation, ingestion, or absorption of radioiodines is development of thyroid cancer (National Research Council 2006). At very high doses (several hundred Gy), the most relevant toxic effect is hypothyroidism rather than thyroid cancer due to the loss of thyroid cell population that accompanies such high doses.

2.3.5. Epidemiological Studies

Most large-scale studies of external exposure to radioiodines involved concurrent exposure to other radionuclides (National Research Council 2006). For example, studies of atomic bomb survivors included concurrent exposure to not only several radionuclides of differing physical forms, but also neutrons. The same applies to studies of nuclear

power plant accidents. Additionally, when radioiodines are located outside of one's body, there is no organ specificity. As a result, identifying an effect that is specific to external exposure of radioiodines (and yet not applicable to external ionizing-radiation sources of similar emission spectra in general) is not meaningful.

Data concerning risk of thyroid cancer as a result of internal exposure to radioiodines, mainly ^{131}I, come mostly from therapeutic and diagnostic scenarios/studies. Such studies mostly consist of internal exposure of adults receiving doses from 0.5 Gy up to as high as 100 Gy; these studies don't provide substantial evidence of increases in thyroid cancer incidence (for non-childhood exposure) due to a lack of consistent results between different studies (National Research Council 2006). Environmental exposure studies such as those focused on weapons testing at Nevada Test Site (Kerber 1993), Bikini Atoll / Marshall Island (Conard 1984), and the Hanford Site production facility (Davis 2004), showed a similar lack of consistency in findings.

In contrast to the comparatively murky data for adult exposure to radioiodines, follow-up studies on the Chernobyl accident showed a marked increase in thyroid cancer incidence among those exposed as children (Mettler 1996, Williams 2003, Kikuchi 2004).

2.3.6. Protective Measures

"Iodide/Iodine prophylaxis" or "thyroid blockade" is a prophylactic method that protects the thyroid gland against radioiodines by redirecting the radioiodines away from the target organ and into the kidneys where they are subsequently excreted in urine. To accomplish this, a thyroid-saturating dose of stable iodide is ingested such that the activity of the sodium-iodide symporter used by thyroid follicular cells decreases to a level where a large majority of any further ingested iodide is simply routed to the kidneys

and excreted rather than absorbed by the thyroid (Hosten 2012). Timed appropriately, this prophylactic measure can prevent a large percentage of thyroid dose that would otherwise be received (Blum 1967).

To represent thyroid blockade when calculating absorbed dose due to internal exposure to radioiodines, the latest available iodine biokinetic model by Leggett reduces the value of a transference coefficient that represents the organification of iodide in the thyroid, which has a baseline age-independent value of 95 day^{-1} (Leggett 2017). For modeling complete thyroid blockade, the transference coefficient is set to zero. Under such parameters, modeling shows that thyroid blockade reduces radioiodine dose to all affected organs except the stomach, for which there is a moderate increase in dose (Leggett 2017). Thyroid blockade is usually incorporated by use of the stable compound Potassium Iodide (KI); this is colloquially referred to as “KI Prophylaxis.”

Because dietary levels of iodine affect the activity of the sodium-iodide symporter in thyroid follicular cells, the effectiveness of thyroid blockade at a fixed prophylactic dose can vary depending on the pre-exposure dietary levels of iodine. When dietary levels of iodine are insufficient for production of T3 and T4, the thyroid enlarges and absorbs more iodine from the blood compared to conditions of euthyroidism. As a consequence, thyroid blockade is less protective at a fixed prophylactic dose if dietary levels of iodine are low prior to exposure (Zanzonico 2000).

Chapter 3. Methods and Materials

3.1. Source Term

Because this assessment involves risk of thyroid cancer and its potential reduction, relevant radioisotopes under consideration are those whose target organ is the thyroid. Iodine and its isotopes all target the thyroid, and all isotopes except ^{127}I are radioactive. Radioactive iodines are the most significant regarding potential thyroid dose from a radiological release involving fission of heavy atoms, as was especially seen at Fukushima (IAEA 2015). Table 3.1. summarizes characteristics of several radioactive isotopes of iodine that are produced by nuclear fission.

Table 3.1. Characteristics of radioactive isotopes of iodine produced by nuclear fission (Knolls Atomic Power Lab 2010, MIRD 1975).

Characteristics of Fission-Produced Radioactive Iodine Isotopes			
Mass Number	Half-life	^{235}U Fission Yield (%)	Thyroid Absorbed Dose per Unit Cumulated Activity in the Thyroid (rad/μCi-hr)
125	59.4 d	0.03	3.00E-03
126	12.89 d	0.06	1.80E-02
129	1.57E+07 y	0.54	7.10E-03
130	12.36 h	1.81	3.90E-02
131	8.023 d	2.89	2.20E-02
132	2.283 h	4.31	6.00E-02
133	20.8 h	6.70	4.60E-02

Only one radioisotope of iodine, ^{131}I, was considered for this assessment as the principle hazard. Other isotopes of iodine could be included, but only ^{131}I has substantial dispersion and uptake potential due to its long half-life and moderately high fission yield. Its ^{235}U fission yield guarantees that it is produced in moderate quantities inside of ^{235}U fission reactors operating for commercial power production.

The basis for the magnitude of ^{131}I release as the source term was rooted in historical radiological incidents in which there were substantial releases of radioactive

iodine from a nuclear power plant. Historical radiological incidents established a plausible magnitude of ^{131}I release for the proposed release scenario of this assessment.

The historical incidents considered here were those that occurred at Chernobyl and Fukushima. The Chernobyl accident, while certainly a substantial release of ^{131}I, does not wholly represent the scenario of a release in Louisiana due to differences of design between United States' reactors and Chernobyl's RMBK-type reactor (National Research Council 2004); Chernobyl's RMBK-type reactor used flammable graphite as a neutron moderator and did not have a containment vessel (NRC 1987). The Fukushima accident is more relevant because the power plant's general design is similar to that of United States' reactors, in that both use water as a neutron moderator and have a containment vessel (IAEA 2015). The magnitude of core inventory release from Fukushima could plausibly occur at a United States facility if a similarly low-probability beyond-design-basis event were to occur.

For this assessment, a nuclear power plant in Louisiana was selected as the release location. Three nuclear power plants are located in or immediately adjacent to Louisiana: River Bend, Waterford 3, and Grand Gulf. Of those three, River Bend is the only power plant whose reactor is the same type as Fukushima's (boiling water reactor); it also is located near the highly populated Baton Rouge metropolitan area. Having the release point located near a high-population area enables a worst-case conservative model regarding numbers of potentially exposed individuals. Therefore, the reactor building at River Bend was chosen as the release point.

With bases selected for the magnitude and location of release, the source term (i.e. the release magnitude and rate) was established by assuming the same severity as the

historical accident coming from the selected release point. The severity of the historical accident was categorized as the percentage of ^{131}I inventory released. To calculate this percentage, the total inventory of ^{131}I present in the reactors at Fukushima prior to their discharge was estimated using (Lamarsh 2001)

$$\alpha_i = 8.46 \times 10^5 \cdot P_t \cdot \gamma_i = 8.46 \times 10^5 \cdot \left(\frac{P_e}{\varepsilon}\right) \cdot \gamma_i \quad [2]$$

where α_i is the radionuclide inventory (in Ci), P_t is the thermal power generated inside reactor (in MW), γ_i is the fission yield of ^{131}I (unitless), P_e is the electric output power of reactor (in MW), and ε is the efficiency of reactor (unitless). This estimation assumed that the reactor had operated long enough for the radionuclide's activity to reach equilibrium. Table 3.2. shows the estimated ^{131}I inventory in Ci and Bq using Eq. 2 for γ_i = 0.0289 and an assumption of ε = 0.33 for the boiling water reactor.

Table 3.2. Inventory calculation for the 3 reactors (units) at Fukushima that released radioactive iodine.

Fukushima ^{131}I Inventory Calculation				
Value		Unit 1	Unit 2	Unit 3
Electric Power Output (P_e)	MW	460	784	784
Efficiency (ε)	%	33	33	33
Thermal Power in Reactor (P_t)	MW	1394	2376	2376
Reactor ^{131}I Inventory (α_i)	Ci	3.4E+07	5.8E+07	5.8E+07
	Bq	1.3E+18	2.1E+18	2.1E+18
Total ^{131}I Inventory	Ci	1.5E+08		
	Bq	5.6E+18		

Several studies of Fukushima have estimated the amount of ^{131}I that was released. The mean of the estimates of such studies was 144 PBq (IAEA 2015). Consequently, the fraction of ^{131}I inventory released at Fukushima was

$$\text{Release as percent of } ^{131}\text{I inventory} = \frac{144 \times 10^{15}\ \text{Bq}}{5.6 \times 10^{18}\ \text{Bq}} \times 100 = 2.6\% \quad [3]$$

For River Bend operating at its licensed capacity of 3091 MW thermal (NRC 2018), the corresponding hypothetical fractional release was calculated using (Lamarsh 2001)

$$Q = \alpha_i \cdot f = [8.46 \times 10^5 \cdot P_t \cdot \gamma_i] \cdot f \quad [4]$$

where Q is the total ^{131}I emission (in Ci), α_i is the radionuclide inventory (in Ci), P_t is the thermal power generated inside reactor (in MW), γ_i is the fission yield of radionuclide (unitless), and f is the fraction of inventory released (unitless). The total emission Q was equal to 7.3×10^{16} Bq.

Assuming that the total emission is released over an amount of time similar to the period over which a majority of Fukushima's inventory was released, approximately 4 days, then the hypothetical emission rate Q' was 1.8×10^{16} Bq/day, or 2.1×10^{11} Bq/s. The emission rate Q' was the source term for the hypothetical accident scenario modeled in this assessment, representing the release rate of ^{131}I from River Bend. The emission rate was assumed to be constant for purposes of environmental transport (see Section 3.2). When calculating dose, this value was subdivided to account for the proportion of gaseous iodine to particle iodine (see Section 3.4).

3.2. Environmental Transport

Because the duration of the emission is assumed to be 4 days, this hypothetical scenario represented an acute, short-term release. Additionally, the potential transit time of emitted effluent was short (hours) compared to the duration of the emission (days) based upon local wind speed data that is discussed later in this section. Transit time of the effluent, relative to the duration of its emission, is important to identify prior to selecting an environmental model because it determines whether the release is a puff or

plume. Generally, if the release duration of the effluent is short compared to the transit time, then it's a puff; otherwise, it's a plume (Pasquill 1984, Till 2008).

Because the potential transit time of the effluent was short compared to the duration of the emission, a Gaussian plume model was an appropriate choice for a transport model. An additional advantage of using a Gaussian plume model was that it provided results that were obtainable without significant computational power. The Gaussian plume model used in this assessment was (Till 2008)

$$C = \frac{Q'}{2\pi\mu\sigma_y\sigma_z}\exp\left[-\frac{1}{2}\left(\frac{y^2}{{\sigma_y}^2}\right)\right]\cdot\left\{\exp\left(-\frac{1}{2}\left[\frac{\left(z-h_p\right)^2}{{\sigma_z}^2}\right]\right)+\exp\left(-\frac{1}{2}\left[\frac{\left(z+h_p\right)^2}{{\sigma_z}^2}\right]\right)\right\}$$
$$\cdot\exp\left(-\frac{0.693}{\mu T_{1/2}}x\right) \qquad [5]$$

where C is concentration in air, Q' is the source term or emission rate, μ is wind speed, h_p is effective stack height, $T_{1/2}$ is the ^{131}I half-life, x is downwind distance, y is crosswind distance, z is vertical distance (fixed height at which concentration is calculated), and σ_y and σ_z are the standard deviations of a Gaussian distribution in the crosswind and vertical directions, respectively. Eq. 5 assumes that the concentration is reflected into the atmosphere when it encounters the ground (Till 2008). The last exponential term of Eq. 5 accounts for radioactive decay of ^{131}I. Values of terms in the Gaussian plume model are summarized in Table 3.3.

The emission rate, Q', is the source term that was calculated previously (see Section 3.1). The height at which concentration in air was calculated, z, was 1.5 meters (5 feet) because human intake of the radionuclide occurs near head-height.

For the effective stack height, h_p, a constant value of 100 m was based upon evaluations of the Fukushima accident, where the stack height ranged from

approximately 20 to 150 meters depending on the mode of release (Korsakissok 2013). For the 20 to 150 m range of stack height, the value of 100 m used for h_p was somewhat arbitrary because the transport model was insensitive to changes in effective stack height. This was determined by holding other transport variables constant, varying the effective stack height within a 20 to 150 m range, and observing changes in transport.

Table 3.3. Summary of values used for the Gaussian plume model.

Term	Description	Value	Unit
Q'	Emission rate	2E+11	Bq/s
μ	Wind speed	6	m/s
h_p	Effective stack height	100	m
$T_{1/2}$	^{131}I half-life	8.023	day
z	Observation height	1.5	m
σ_y	Crosswind standard deviation	Dependent on downwind distance*	m
σ_z	Vertical standard deviation		

*For an assumed atmospheric stability category.

For the wind speed, μ, a constant value of 6 m/s was chosen based upon 2018 climatology data from the National Oceanic and Atmospheric Administration (NOAA 2018). This value represented a wind speed that was higher than typical monthly averages for the Louisiana area. In 2018, monthly average wind speeds ranged from ~3 m/s to ~5 m/s (NOAA 2018). A higher-than-monthly-average wind speed was used to compensate for two factors. The first factor was the Gaussian plume model's assumption of steady-state conditions for a constant atmospheric stability. For steady-state conditions and constant atmospheric stability, lower wind speeds generated higher concentrations for a given downwind distance but resulted in excessive travel of the plume to distances where the model, in its simplest form here, is unlikely to be reliable. The second factor was the height of approximately 1.5 meters from which the NOAA wind data was measured (NOAA 2018). Determination of the increase in wind speed at

the plume's stack height of 100 meters, relative to the wind speed measurement height at 1.5 meters, was estimated using a wind profile power law relationship that depended principally on an assumed "atmospheric stability category" that is discussed later in this section. For the wind profile power law relationship detailed in the EPA's Industrial Source Complex 3 (ISC3) dispersion model (EPA 1995), a 4 m/s wind speed at a height of 1.5 m corresponded to 6 m/s at 100 m. A wind speed of 6 m/s was adequately representative of the area under consideration based upon local climatology data and the requisite increase in wind speed at the stack release height relative to the height of wind speed measurement.

The dispersion coefficients σ_y and σ_z were calculated using equations from the EPA's ISC3 dispersion model (EPA 1995), which contain equations that have been fitted to measured and extrapolated plume dispersion data from Pasquill (Pasquill 1961). The fitted equations for σ_y and σ_z depend on the "atmospheric stability category" of the Pasquill curves. Atmospheric stability categories depend on wind speed range and sun insolation during daytime or cloudiness during nighttime. Moderate or strong sun insolation during daytime was assumed, as both resulted in the same atmospheric stability category. For a 6 m/s wind speed and moderate or strong sun insolation during daytime, corresponding to atmospheric stability category C (Pasquill 1961), the equations for σ_y and σ_z were

$$\sigma_y = 465.11628x * \tan(\ 0.017453293[12.5 - 1.0857\ln(x)]\ ) \quad [6]$$

and

$$\sigma_z = 61.141x^{0.91465} \text{ for } \sigma_z \leq 5000 \quad [7]$$

where x is downwind distance (in km), and σ_y and σ_z are dispersion coefficients (in m). The dispersion coefficients from Pasquill were for an approximate 10-minute averaging time (Pasquill 1961), which is less than this hypothetical release's duration of 96 hours. The coefficients could have been adjusted to compensate for that difference by using an empirical formula (Gifford 1982), but that adjustment would have resulted in further diffusion of the plume. It was a conservative approach to exclude the empirical adjustment because, by excluding it, the resultant plume covered a larger area. The Gaussian plume model used in this assessment was calculated with the software MATLAB R2018a by MathWorks.

3.3. Population Exposure Factors

The plume of ^{131}I was assumed to travel along a worst-case path, which was defined as the straight-line path from the radionuclide release point that results in the largest potential risk to the exposed population. This assessment defined a metric called cumulative susceptibility to excess risk (CSER) to determine which populations near the radionuclide release point were most susceptible to excess risk due to ^{131}I exposure. The CSER for a population P was defined as

$$\mathrm{CSER_P} = \sum_i (\alpha \times \beta)_{i,\mathrm{males}} + \sum_i (\alpha \times \beta)_{i,\mathrm{females}} \quad [8]$$

where $\mathrm{CSER_P}$ is cumulative susceptibility to excess risk for population P, α_i is ERR per Gy of thyroid dose for demographic i of population P, and β_i is the size of demographic i (i.e. number of people). The CSER does not account for varying population density within a given area or that doses received by individuals within the population vary according to several factors.

The demographic categories for this assessment comprised age groups from <5 years to 39 years of age at exposure. Individuals over this age were not included in the population because the risk of radiation-induced thyroid cancer, the risk endpoint for this assessment, is low (National Research Council 2006). In older individuals, the principal risk is destruction of thyroid tissue rather than thyroid cancer. This is illustrated by the FDA's recommendations of KI prophylaxis as a thyroid protective measure, whereby the intervention level is a projected thyroid dose of ≥500 cGy for those over 40 years old versus ≥10 cGy for those aged 18 to 40 years at the time of exposure (FDA 2001).

The sizes of the demographics, β_i, in the Louisiana parishes surrounding the River Bend nuclear power plant were calculated from 2017 demographic estimates derived from 2010 census data (ACS 2018). Population density within each parish was assumed to be uniform. Demographics were defined for 8 age groups for both males and females; the age groups were <5, 5-9, 10-14, 15-19, 20-24, 25-29, 30-34, and 35-39 years old.

For determining the ERR per Gy for each demographic, α_i, the BEIR VII committee's risk model for thyroid cancer was used (National Research Council 2006). α_i was calculated as

$$\alpha_{i,\text{males}} = \frac{1}{5}\sum_{e\in i} 0.53 * \exp[-0.083(e-30)] \quad [9]$$

for males and

$$\alpha_{i,\text{females}} = \frac{1}{5}\sum_{e\in i} 1.05 * \exp[-0.083(e-30)] \quad [10]$$

for females, where the e are the ages at exposure in years within each demographic.

3.4. Conversion to Dose and Risk

As discussed in Section 2.3.2, inhalation dose is the dominant pathway for exposure following a release of ^{131}I from a nuclear power plant; the ingestion pathway is constrained by interdiction procedures that halt distribution of contaminated food and drink (see Section 2.3.2). Consequently, only the inhalation pathway was included in calculation of dose.

To determine the amount of ^{131}I inhaled by exposed populations, ventilation parameters and time expenditures (hours spent per day at some level of physical activity) from ICRP Publication 71 were used (ICRP 1995). Because this assessment modeled a worst-case scenario where no evacuation or sheltering occurs, it was assumed that populations are exposed for 24 hours per day, totaling to 96 hours of exposure over the scenario's release duration of 4 days. The total intake of ^{131}I for each demographic was calculated as

$$I_i = BR_i \times TE_i \times HE \times C \quad [11]$$

where I_i is the total intake of ^{131}I for demographic i (in Bq), BR_i is the breathing rate for demographic i (in m^3/hr), TE_i is the normalized time expenditure for demographic i (unitless), HE is the exposure time (in hours), and C is the concentration of ^{131}I in air (in Bq/m^3).

For relating inhalation of ^{131}I to dose, 80% of the emitted iodine was assumed to be in the form of elemental iodine as a gas, and 20% was an aerosol with a 1 μm activity median aerodynamic diameter (AMAD), which is similar to observations at Fukushima (IAEA 2015). Both forms of iodine were assumed to transport identically with regard to the environmental transport model because gravitational settling and deposition effects,

which are the principal differences between atmospheric transport of particles and gases (Brenk et. al 1983), were not incorporated into the transport model. This assumption likely overestimated airborne concentrations due to a lack of removal of iodine from the plume as it was transported (Lakes 2019).

Sex-averaged committed equivalent dose coefficients from ICRP Publication 71 were used to calculate thyroid committed equivalent dose for the ^{131}I inhalation pathway. Because ^{131}I emits only photons and beta particles (Knolls Atomic Power Lab 2010), whose radiation weighting factors are equal to 1 (ICRP 2007), the thyroid committed equivalent dose given by the dose coefficients in Sv was equal to the thyroid absorbed dose in Gy. This conversion was necessary because the appropriate unit for the thyroid cancer risk model used in this assessment is Gy, not Sv (National Research Council 2006). Dose coefficients used for each demographic are summarized in Table 3.4. Dose was calculated identically for males and females; the dose to males and females per intake are about the same because both intake and body mass are about 20% lower for females (ICRP 1995). Additionally, iodine retention does not appear to differ substantially between sexes (Leggett 2017).

Table 3.4. Dose coefficients used for each demographic (ICRP 1995).

Cohort	Age Range (Years)	Median Age (Years)	Gaseous Thyroid Dose Coeff. for Median Age (Gy/Bq)	Aerosol (AMAD=1μm) Thyroid Dose Coeff. for Median Age (Gy/Bq)
1	<5	2	3.20E-06	1.40E-06
2	5-9	7	1.90E-06	7.30E-07
3	10-14	12	9.50E-07	3.70E-07
4	15-19	17	6.20E-07	2.20E-07
5	20-24	22	3.90E-07	1.50E-07
6	25-29	27	3.90E-07	1.50E-07
7	30-34	32	3.90E-07	1.50E-07
8	35-39	37	3.90E-07	1.50E-07

Because the Gaussian plume model can calculate radionuclide concentrations down to arbitrarily small values, a cutoff value was needed to define the plume boundary. Louisiana's Peacetime Radiological Response Plan states that evacuation is recommended for areas where the exposed population is anticipated to receive a thyroid committed dose equivalent (CDE) ≥5000 mrem (Louisiana Department of Health 2016). The plume boundary concentration (BC) was calculated using the concentration of ^{131}I (80% gaseous and 20% 1 μm AMAD) that resulted in a thyroid CDE of 5000 mrem (0.05 Sv) for a person <5 years of age engaged in light exercise for the entirety of the hypothetical release (4 days, or 96 hours). The BC was calculated as

$$\mathrm{BC} = \frac{\text{Thyroid CDE Limit}}{\text{CDE Coefficient}} \times \frac{1}{\text{Intake}} \qquad [12]$$

and when parameters from ICRP Publication 71 (ICRP 1995) were applied,

$$\mathrm{BC} = \frac{0.05\ \mathrm{Sv}}{3.23 \times 10^{-6} * 0.8\ +\ 1.4 \times 10^{-6} * 0.2\ \frac{\mathrm{Sv}}{\mathrm{Bq}}} \times \frac{1}{0.35 \frac{\mathrm{m}^3}{\mathrm{hr}} * 96\ \mathrm{hr}} = 520\ \mathrm{Bq/m^3}$$

which was rounded down to 500 Bq/m^3 for convenience, to become the cutoff value that defined the plume boundary.

Parish-specific uniform population densities were assumed when calculating thyroid absorbed dose, ERR, and Lifetime Attributable Risk (LAR, see Section 2.2). Because of that assumption, values of dose and risk were calculated for every potential location within the plume. Thyroid absorbed dose was calculated using the ICRP dose coefficients shown in Table 3.4. ERR was calculated using the BEIR VII thyroid cancer risk model from Eq. 1. Values of ERR from this assessment were plotted as averages over 5-year age range groups and included the expected value, upper bound, and lower bound for each data point.

LAR was calculated as

$$LAR(D,e) = \sum_{a=e+L}^{100} ERR(D,e) \times \lambda_I^c(a) \times \frac{S(a)}{S(e)} \quad [13]$$

where ERR is the excess relative risk, D is the absorbed dose, a is the attained age, e is the age at exposure, L is the latent period (assumed to be 5 years), $\lambda_I^c(a)$ is the age- and sex-specific cancer incidence rate, $S(a)$ is the probability of surviving to age a, and $S(e)$ is the probability of surviving to age e. The fraction $\frac{S(a)}{S(e)}$ is the probability of surviving to age a conditional on survival to age e.

Values of $\lambda_I^c(a)$ were obtained from 2011-2015 Surveillance, Epidemiology, and End Results (SEER) registries for all stages (malignant) of thyroid cancer (NAACCR 2018). Louisiana-specific thyroid cancer incidence, when not suppressed, was used. When Louisiana-specific incidence was suppressed, the United States average was used. For females aged less than one-years old, both the Louisiana and United States average incidence was suppressed, so a value of 0.01 per 100,000 was assumed. This assumption was intended to represent a non-zero incidence rate; for comparison to other rates, the assumed incidence rate was lower than all other demographic incidence rates, with the closest being 0.02 per 100,000 for males aged two-years old (NAACCR 2018).

Because the incidence rates from SEER registries are given over a range of ages rather than for single years of age, linear interpolation was used to determine incidence rates for single years of age. For ages 85 and up, linear interpolation was not used, and instead the constant incidence rate for ages 85 and up (given by SEER data) was used. Values of S(a) and S(e) for single years of age were obtained from 2015 Life Tables (Arias 2018). Values of LAR from this assessment were plotted as averages over 5-year

age range groups and included the expected value, upper bound, and lower bound for each data point.

Excess lifetime thyroid cancers were calculated by multiplying percentile values of the demographic-specific LAR distribution by the total number of exposed people within a given demographic. To calculate the total number of exposed people, the assumed parish-specific uniform population densities were multiplied by the area of plume coverage over the affected parishes. The area of plume coverage for each parish was approximated by dividing the plume into 60 rectangular segments and then summing the area of segments located within the parish of interest. To calculate the total number of exposed people within each demographic, parish-specific proportions of each demographic were assumed to hold constant over the plume area. For example, if 3% of a parish's population was males aged 10-14, then it was assumed that 3% of the population within an exposed area of that same parish was males aged 10-14.

3.5. Reduction of Risk

For modeling thyroid cancer risk reduction by KI prophylaxis, the thyroid absorbed dose was multiplied by a reduction constant. The value of the constant was determined by two approaches.

The first approach, termed the "ideal model," used results from a biokinetic model for iodine in humans (Leggett 2017), where the thyroid was considered blocked during the entirety of exposure to ^{131}I. To model complete thyroid blockade, a transference coefficient of the biokinetic model that represents the organification of iodide in the thyroid was set to zero. Reduction of thyroid dose was calculated from the ratio of thyroid

CDE per Bq with complete thyroid blockade versus without thyroid blockade for intravenous injection of ^{131}I into an adult male (Leggett 2017).

The second approach, termed the “Poland model,” used results from an evaluation of approximately 17.5 million individuals in Poland who were administered KI in response to the Chernobyl accident (Nauman 1993). In the evaluation, thyroid doses to the exposed population were reconstructed, and the dose reduction due to thyroid blockade was estimated in consideration of ingestion and inhalation pathways and the timing of KI administration relative to exposure to ^{131}I (Nauman 1993).

Chapter 4. Results and Discussion

Figure 4.1. shows the downwind and crosswind concentration of airborne ^{131}I from a release point located at the origin of the plot. Figure 4.1. was generated using MATLAB R2018a by MathWorks, and the resolution of the plot is 25 meters (i.e. there is one data point of concentration every 25 meters).

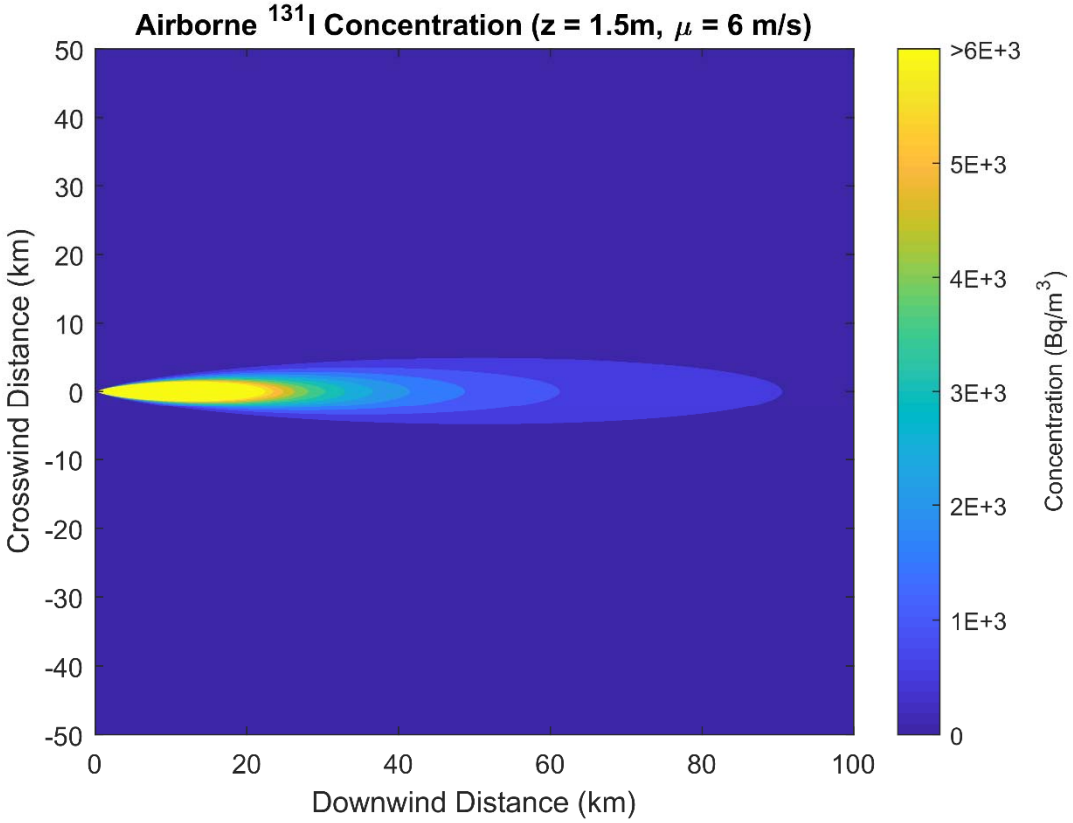

Figure 4.1. Steady-state concentration of airborne ^{131}I for a wind speed of 6 m/s, at an observation height of 1.5 m, due to an emission rate of $2*10^{11}$ Bq/s.

The CSER for parishes within a 50-mile radius for the release point, sorted by descending CSER, is shown in Table 4.1. The results from Table 4.1. indicated that the worst-case (highest CSER) straight-line plume path consists of exposure to East Baton Rouge, Ascension, East Feliciana, and West Feliciana parish.

Table 4.1. CSER of Louisiana parishes that are within a 50-mile radius of the reactor building of River Bend Nuclear Station.

Louisiana Parish within 50-mile radius of release point	CSER (ERR-Person/Gy)
East Baton Rouge	702377
Livingston	220850
Tangipahoa	214894
Ascension	201030
St. Landry	139430
St. Martin	84462
Avoyelles	61100
Iberville	45027
West Baton Rouge	41269
Point Coupee	31179
Concordia	29706
East Feliciana	23072
West Feliciana	15848
St. Helena	14330

Figure 4.2. shows a Google Earth (Google 2017) overlay of the ^{131}I plume to-scale traveling over its worst-case (highest CSER) path, assuming uniform population density over exposed areas. The plume extends for approximately 90 km (56 mi) from the reactor building of River Bend Nuclear Station, which was the release point for this hypothetical scenario.

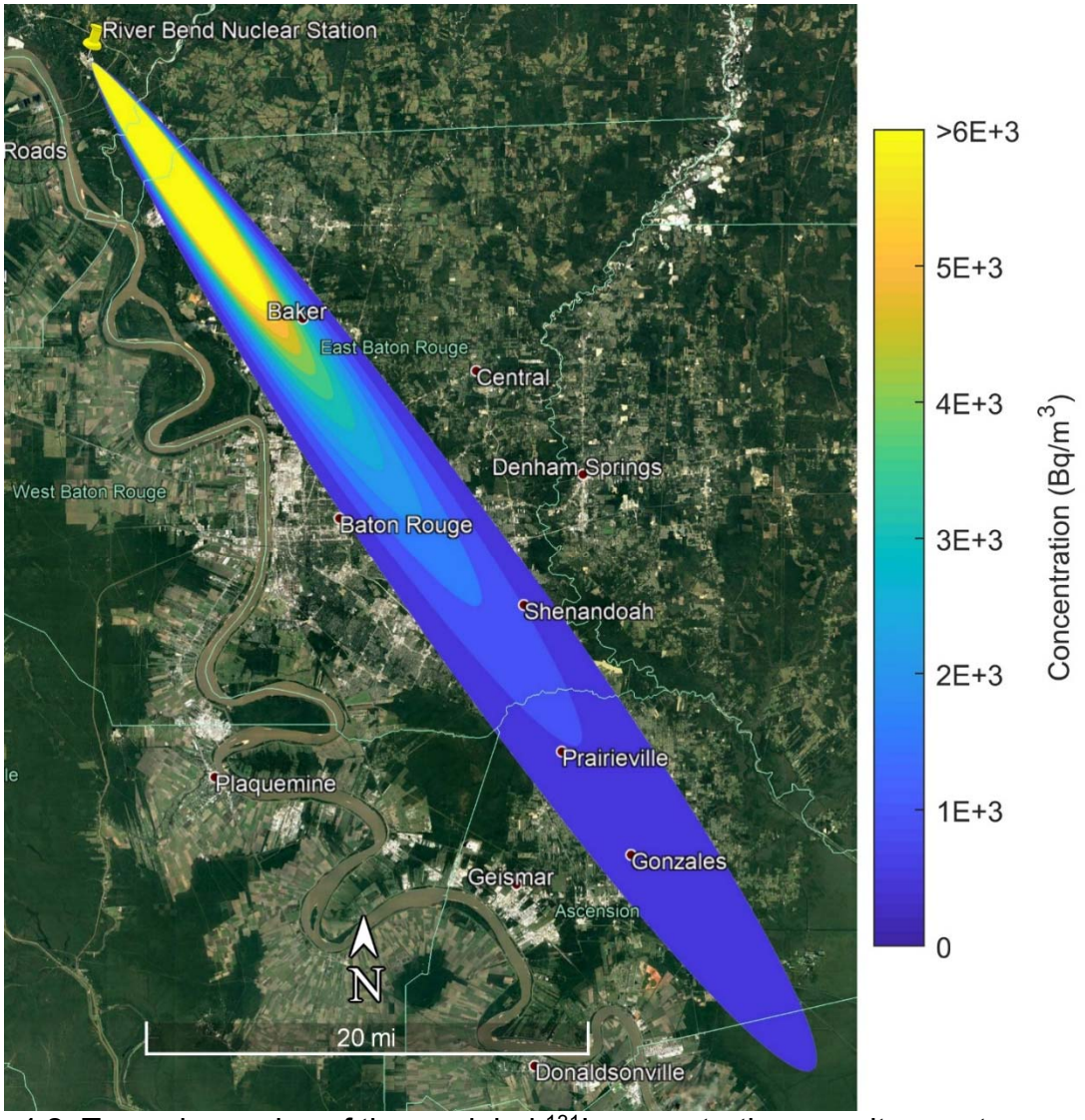

Figure 4.2. To-scale overlay of the modeled ^{131}I concentration over its worst-case path according to the CSER; this assumes uniform population density within each parish. The plume's heading is 144.3 degrees from due north and extends for approximately 90 km (56 mi) from the release point. The source is located at latitude 30°45'26.67"N, longitude 91°19'54.89"W (Google 2017).

Table 4.3. summarizes the number of exposed people within the plume path. As discussed in Section 3.4, the numbers of exposed people within each demographic were used when excess cancers were calculated. Due to the Baton Rouge population, the largest number of people exposed were those between 20 and 24 years of age.

Table 4.3. Total number of exposed individuals within the worst-case plume path.

Total Number of Exposed Individuals		
Age	Sex	Number Exposed*
<5	Male	6,261
	Female	6,055
5-9	Male	6,079
	Female	5,865
10-14	Male	5,923
	Female	5,796
15-19	Male	6,414
	Female	6,509
20-24	Male	9,020
	Female	9,192
25-29	Male	7,178
	Female	6,969
30-34	Male	6,395
	Female	6,542
35-39	Male	5,896
	Female	6,310
All		106,404

*The number of significant figures shown is not meant to imply precision. Values shown are the resultant product of plume area coverage and parish-specific uniform population densities.

4.1. Thyroid Absorbed Dose

Figure 4.3. plots thyroid absorbed dose in cGy due to inhalation of ^{131}I for each age group for both sexes combined, as a function of age at exposure. These are composite values for each age group, calculated from doses to individuals within all possible locations of the plume. Figure 4.3. indicated that this hypothetical exposure scenario would likely warrant an evacuation from the affected areas because the median thyroid dose for those aged <15 years old meets or exceeds 5 cGy, which corresponds to Louisiana's 5-rem thyroid CDE threshold for recommendation of evacuation (Louisiana Department of Health 2016). The dose distribution for each age group was clumped towards lower doses, with high-dose tails caused by the assumption of uniform population density (i.e. there was at least one person of each age group in the highest-

concentration areas of the plume). Table A.1. provides the percentile values of dose that comprise Figure 4.3.

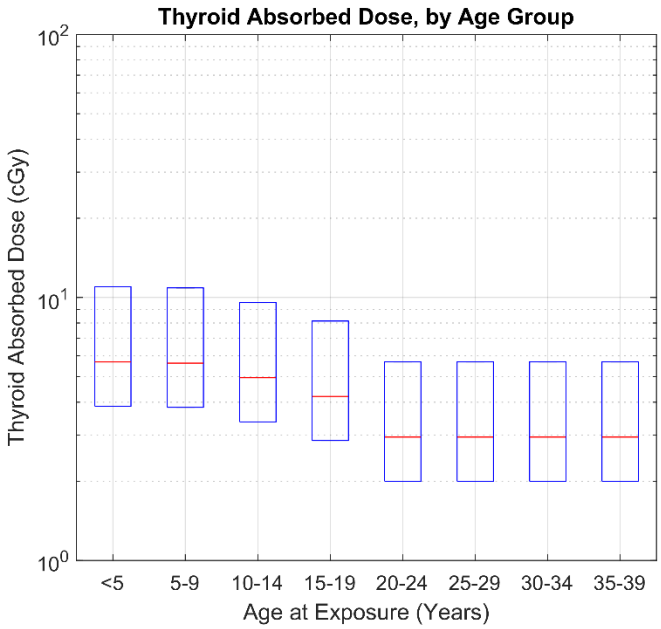

Figure 4.3. Thyroid absorbed dose as a function of age at exposure due to inhalation of ^{131}I. Horizontal lines of the boxes represent 25th, 50th, and 75th percentiles.

For comparison of these results to the Fukushima accident upon which the exposure scenario is based, the majority of emergency workers (17,804 of 19,561; 91%) who assisted during the Fukushima accident were estimated to have received thyroid absorbed doses of less than 10 cGy (IAEA 2015). Concerning thyroid dose to the general public from the Fukushima accident, an assessment from the World Health Organization estimated a typical dose band to those in the Fukushima Prefecture of 1-10 cGy, with one particular location having an estimated 10-20 cGy dose to infants (IAEA 2015). The distribution of thyroid dose shown in Figure 4.3. generally tracked with the distribution of thyroid dose from the Fukushima accident, which suggested that the results were reasonable for the hypothetical exposure scenario.

4.2. Thyroid Cancer Risk

Figure 4.4. plots ERR for each age group for both sexes. As expected, females showed a higher ERR than males because the thyroid cancer risk model used in this assessment predicted a higher ERR per Gy for females than males (see Eq. 1), and dose was calculated independent of sex. The majority of ERR was below a value of 1, which meant that most of the exposed population had less than a 100% increase (doubling) of their baseline thyroid cancer risk. The only demographic that exceeded an ERR of 1 in their interquartile range was females <10 years of age. In contrast, people exposed at >19 years of age had increases in baseline risk that were generally below 20%, indicating that risk reduction interventions (such as KI prophylaxis) should prioritize young populations. Table A.2. provides the percentile values of ERR that comprise Figure 4.4.

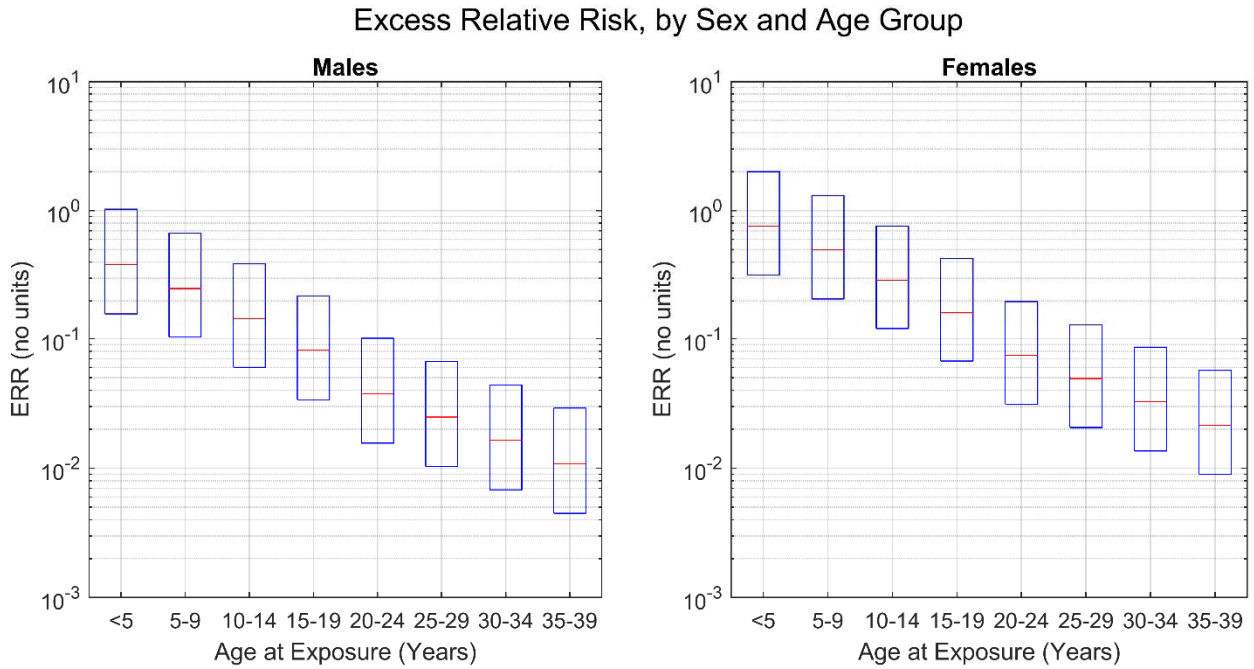

Figure 4.4. ERR as a function of sex and age at exposure due to inhalation of ^{131}I. Horizontal lines of the boxes represent 25th, 50th, and 75th percentiles.

Figure 4.5. plots LAR per 1,000 people exposed for each age group for both sexes (see Sections 2.2 and 3.4 for definition of LAR). Figure 4.5. indicated that females had a LAR that was larger than males by a factor of about 5, meaning that excess lifetime thyroid cancer incidence due to exposure was 5 times larger for females than males. Table A.3. provides the percentile values of LAR that comprise Figure 4.5.

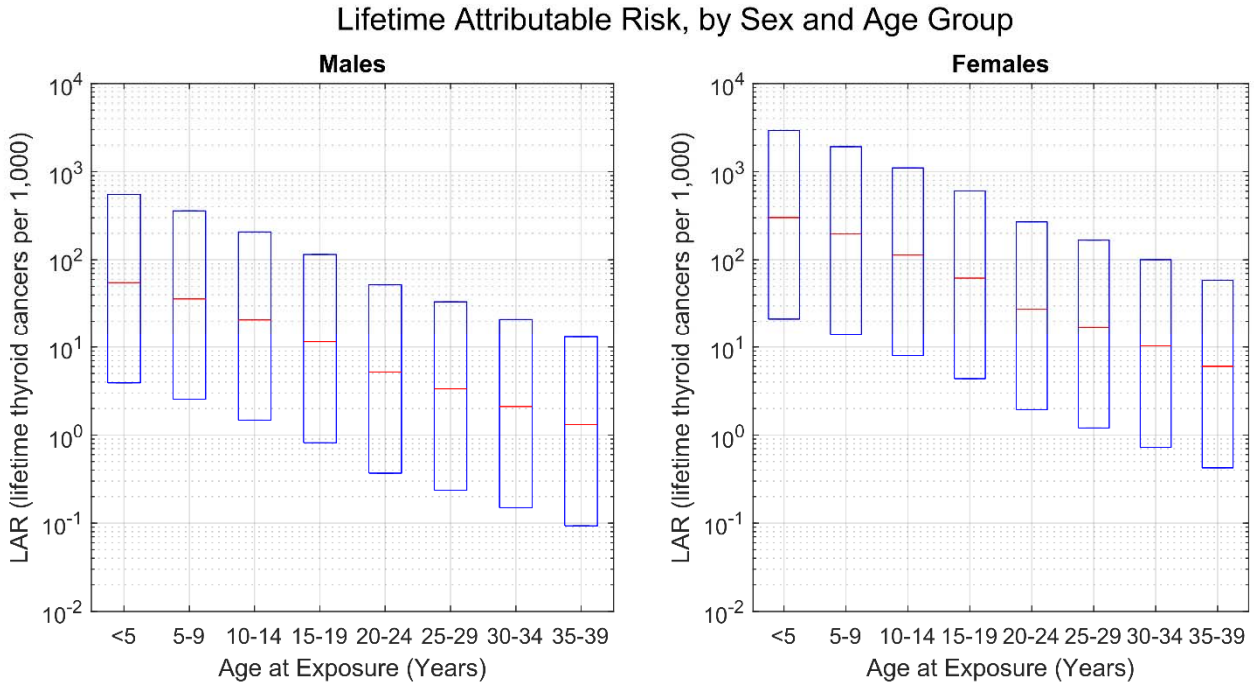

Figure 4.5. LAR (per 1,000) as a function of sex and age at exposure, assuming a 5-year latent period for radiation-induced thyroid cancer. Horizontal lines of the boxes represent 25th, 50th, and 75th percentiles.

Females were expected to have a larger LAR than males for three reasons. The first reason was that females generally have a higher baseline thyroid cancer risk than males (NAACCR 2018), meaning that their excess absolute risk (EAR, see Section 2.2) for a given value of ERR would be larger than for males. The second reason was that females generally have a longer life expectancy than males (Arias 2018), so that when LAR was calculated, the high incidence rates of old age were weighted more. The third reason

was that the thyroid cancer risk model used in this assessment predicts a higher ERR per Gy for females than males (see Eq. 1).

4.3. Risk Reduction

For the ideal model approach, which assumes thyroid is blocked for the entirety of exposure to ^{131}I, thyroid dose was reduced by three orders of magnitude (Leggett 2017). The ideal model does not represent a typical dose reduction, but it was helpful to estimate the extent to which cross-irradiation from ^{131}I accumulation in non-thyroidal tissue would impact thyroid dose when the thyroid is blocked.

For the Poland model approach, a retrospective evaluation of populations in Poland that received KI in response to the Chernobyl accident estimated that thyroid blockade reduced thyroid doses by 40% (Nauman 1993). The authors of the evaluation further stated that, had there been timely notification of the accident by Russian authorities, the dose reduction could have been as high as 60% to 70% with early prophylaxis, particularly with respect to inhaled ^{131}I (Nauman 1993).

Table 4.4. shows the number of mitigated excess lifetime thyroid cancers from thyroid blockade for this assessment's hypothetical exposure scenario, as a function of percentiles of LAR. Values in Table 4.4. were presented in the form of their expected value followed by their lower and upper bound in parentheses. As expected, based upon the results of LAR in Figure 4.5., the majority of excess lifetime thyroid cancers mitigated by thyroid blockade were due to females.

The two approaches of dose reduction shown in Table 4.4. illustrated an ideal reduction ("ideal model"), which is unlikely to be achievable in practice, and a plausible reduction ("Poland model") of excess lifetime thyroid cancers. Percentiles of LAR, which

are values of lifetime risk that a percentage of the exposed population was below, were used as representative values that gauged the conservatism of the estimate of mitigated excess thyroid cancers. For example, the number of mitigated excess thyroid cancers for the 75th percentile of LAR was likely an overestimate, because it assumed that 100% of the population has a LAR that 75% of the population was below. As a consequence, the number of mitigated cancers for the 50th percentile of LAR may be a more accurate estimate than other values in Table 4.4. The 50th percentile LAR estimate showed that the expected number of mitigated excess thyroid cancers was around 200 for the "ideal model" and 80 for the "Poland model."

Table 4.4. Number of mitigated excess lifetime cancers via thyroid blockade for LAR percentiles applied to entire demographics.*

LAR Percentile Applied	Ideal Model; Mitigated Thyroid Cancers >99% dose reduction			Poland Model; Mitigated Thyroid Cancers 40% dose reduction		
	Male	Female	Total	Male	Female	Total
25th	22 (5, 82)	114 (30, 426)	136 (35, 508)	8 (1, 33)	47 (12, 172)	55 (13, 205)
50th	33 (7, 122)	168 (46, 626)	201 (53, 748)	13 (4, 50)	68 (19, 251)	81 (23, 301)
75th	62 (15, 235)	326 (87, 1212)	388 (102, 1447)	25 (8, 94)	130 (36, 485)	155 (44, 579)

*Number of significant figures shown is not meant to imply precision. Values shown are the product of demographic-specific LAR percentiles and total number of exposed people within each demographic. Values are presented as their expected value, followed by their lower and upper bound in parentheses.

4.4. Limitations and Future Work

This project had several limitations that contributed to its uncertainty. Foremost, the environmental transport model used in this assessment had several simplifying assumptions, such as a constant emission rate, constant wind speed and direction, and uniform population densities. An improved assessment should incorporate terrain data, weather patterns, varying population densities, and other factors that affect environmental transport. Publicly available geographic information from Geographical

Information Systems data could be incorporated into a transport model. Commercial dispersion software packages, albeit expensive, include such features.

Regarding calculation of excess thyroid cancer risk, the risk model used in this assessment was the preferred model reported in the BEIR VII report (National Research Council 2006). The model was developed using a pooled analysis of data from seven thyroid cancer incidence studies, which included atomic bomb survivors. Most of the data involved external exposure from x-rays rather than internal exposure from ^{131}I (National Research Council 2006), which was the pathway of interest for this assessment. A potentially important modifier of the model, though not well-quantified at this time, is dietary iodine deficiency (Shakhtarin 2003, Cardis 2005). A Louisiana-specific study of urinary iodine excretion could clarify iodine deficiency prevalence among populations used for this assessment. This could be factored into the ERR per Gy for the affected populations, so that the impact on the protective effect of KI prophylaxis could be assessed.

A factor affecting the calculated LAR is the fact that thyroid cancer incidence in Louisiana has been increasing over the past several years (NCI 2019). Because a relative risk (RR) model was used for this assessment, an increase in baseline risk yields a higher LAR for a fixed RR, which in turn would increase the potential number of excess lifetime thyroid cancers induced by the hypothetical event described in this assessment.

Lastly, this assessment addressed only one factor pertaining to the risk management question of whether Louisiana should provide KI pills to its general public. Future work that addresses other factors of this question would be beneficial. The other factors include financial cost; logistics of storage, distribution, and re-stocking of KI pills;

legal issues of widespread administration; and psychosocial ramifications of implementing such a policy. Additionally, future work that models risk reduction from anticipated evacuation and sheltering without thyroid blockade, and an associated comparison to the risk reduction from thyroid blockade without evacuation and sheltering, should aid decision-making for this issue.

4.5. Conclusion

This assessment provided a preliminary screening of the Louisiana-specific benefit of thyroid cancer risk reduction due to thyroid blockade in a hypothetical exposure scenario. Results indicated that thyroid blockade reduced a number of excess lifetime thyroid cancers that was on the order of 80 across approximately 100,000 exposed individuals, though the bounds on this estimate were large. The majority of mitigated excess lifetime thyroid cancers were due to dose reduction in young females. Given these results, more comprehensive assessments of KI distribution in Louisiana may be warranted. By generating these results, people in positions of risk management for Louisiana have access to Louisiana-specific information regarding the risk reduction benefit of thyroid blockade for the general public.

Appendix A. Percentile Data of Dose, ERR, and LAR

Table A.1. Percentiles of Thyroid Absorbed Dose by Age at Exposure

Percentiles of Thyroid Absorbed Dose by Age at Exposure			
Age (Years)	Thyroid Absorbed Dose (cGy)		
	25th	50th	75th
<5	3.86E+00	5.68E+00	1.10E+01
5-9	3.82E+00	5.63E+00	1.09E+01
10-14	3.36E+00	4.95E+00	9.57E+00
15-19	2.86E+00	4.21E+00	8.13E+00
20-24	2.00E+00	2.94E+00	5.69E+00
25-29	2.00E+00	2.94E+00	5.69E+00
30-34	2.00E+00	2.94E+00	5.69E+00
35-39	2.00E+00	2.94E+00	5.69E+00

Table A.2. Percentiles of Excess Relative Risk by Sex and Age at Exposure

Excess Relative Risk (ERR) Percentiles by Sex and Age at Exposure*										
Age (Years)	Sex	ERR (unitless)								
		25th			50th			75th		
		Mean	LB	UB	Mean	LB	UB	Mean	LB	UB
<5	Male	2.11E-01	5.56E-02	7.95E-01	3.10E-01	8.19E-02	1.17E+00	5.99E-01	1.58E-01	2.26E+00
	Female	4.17E-01	1.11E-01	1.55E+00	6.14E-01	1.64E-01	2.28E+00	1.19E+00	3.17E-01	4.41E+00
5-9	Male	1.38E-01	3.64E-02	5.19E-01	2.03E-01	5.35E-02	7.65E-01	3.92E-01	1.03E-01	1.48E+00
	Female	2.73E-01	7.27E-02	1.01E+00	4.01E-01	1.07E-01	1.49E+00	7.76E-01	2.07E-01	2.88E+00
10-14	Male	8.00E-02	2.11E-02	3.02E-01	1.18E-01	3.11E-02	4.44E-01	2.28E-01	6.01E-02	8.59E-01
	Female	1.58E-01	4.22E-02	5.88E-01	2.33E-01	6.22E-02	8.66E-01	4.51E-01	1.20E-01	1.67E+00
15-19	Male	4.49E-02	1.19E-02	1.69E-01	6.60E-02	1.74E-02	2.49E-01	1.28E-01	3.37E-02	4.82E-01
	Female	8.89E-02	2.37E-02	3.30E-01	1.31E-01	3.49E-02	4.86E-01	2.53E-01	6.74E-02	9.39E-01
20-24	Male	2.07E-02	5.47E-03	7.82E-02	3.05E-02	8.06E-03	1.15E-01	5.90E-02	1.56E-02	2.23E-01
	Female	4.11E-02	1.09E-02	1.53E-01	6.04E-02	1.61E-02	2.25E-01	1.17E-01	3.12E-02	4.34E-01
25-29	Male	1.37E-02	3.62E-03	5.16E-02	2.01E-02	5.32E-03	7.60E-02	3.89E-02	1.03E-02	1.47E-01
	Female	2.71E-02	7.23E-03	1.01E-01	3.99E-02	1.06E-02	1.48E-01	7.72E-02	2.06E-02	2.87E-01
30-34	Male	9.04E-03	2.39E-03	3.41E-02	1.33E-02	3.51E-03	5.02E-02	2.57E-02	6.79E-03	9.71E-02
	Female	1.79E-02	4.77E-03	6.65E-02	2.64E-02	7.03E-03	9.79E-02	5.10E-02	1.36E-02	1.89E-01
35-39	Male	5.97E-03	1.58E-03	2.25E-02	8.78E-03	2.32E-03	3.32E-02	1.70E-02	4.49E-03	6.41E-02
	Female	1.18E-02	3.15E-03	4.39E-02	1.74E-02	4.64E-03	6.46E-02	3.36E-02	8.97E-03	1.25E-01

*"LB" indicates lower bound, and "UB" indicates upper bound.

Table A.3. Percentiles of Lifetime Attributable Risk by Sex and Age at Exposure

Lifetime Attributable Risk (LAR) Percentiles by Sex and Age at Exposure*										
Age (Years)	Sex	LAR (per 1,000)								
		25th			50th			75th		
		Mean	LB	UB	Mean	LB	UB	Mean	LB	UB
<5	Male	1.38E+00	3.63E+01	5.19E+02	2.02E+00	5.35E+01	7.64E+02	3.91E+00	1.03E+02	1.48E+03
	Female	7.45E+00	1.99E+02	2.77E+03	1.10E+01	2.93E+02	4.08E+03	2.12E+01	5.66E+02	7.88E+03
5-9	Male	8.99E-01	2.37E+01	3.39E+02	1.32E+00	3.49E+01	4.99E+02	2.56E+00	6.76E+01	9.65E+02
	Female	4.87E+00	1.30E+02	1.81E+03	7.16E+00	1.91E+02	2.66E+03	1.38E+01	3.69E+02	5.14E+03
10-14	Male	5.19E-01	1.37E+01	1.96E+02	7.64E-01	2.02E+01	2.88E+02	1.48E+00	3.90E+01	5.57E+02
	Female	2.80E+00	7.47E+01	1.04E+03	4.12E+00	1.10E+02	1.53E+03	7.97E+00	2.13E+02	2.96E+03
15-19	Male	2.88E-01	7.60E+00	1.09E+02	4.23E-01	1.12E+01	1.60E+02	8.18E-01	2.16E+01	3.09E+02
	Female	1.54E+00	4.10E+01	5.71E+02	2.26E+00	6.03E+01	8.40E+02	4.37E+00	1.17E+02	1.62E+03
20-24	Male	1.30E-01	3.43E+00	4.91E+01	1.91E-01	5.06E+00	7.22E+01	3.70E-01	9.77E+00	1.40E+02
	Female	6.83E-01	1.82E+01	2.54E+02	1.00E+00	2.68E+01	3.73E+02	1.94E+00	5.18E+01	7.22E+02
25-29	Male	8.35E-02	2.21E+00	3.15E+01	1.23E-01	3.25E+00	4.64E+01	2.38E-01	6.28E+00	8.97E+01
	Female	4.24E-01	1.13E+01	1.57E+02	6.24E-01	1.66E+01	2.32E+02	1.21E+00	3.22E+01	4.48E+02
30-34	Male	5.27E-02	1.39E+00	1.99E+01	7.75E-02	2.05E+00	2.92E+01	1.50E-01	3.96E+00	5.65E+01
	Female	2.55E-01	6.80E+00	9.47E+01	3.75E-01	1.00E+01	1.39E+02	7.25E-01	1.93E+01	2.69E+02
35-39	Male	3.28E-02	8.67E-01	1.24E+01	4.83E-02	1.28E+00	1.82E+01	9.34E-02	2.47E+00	3.53E+01
	Female	1.49E-01	3.98E+00	5.54E+01	2.20E-01	5.86E+00	8.16E+01	4.25E-01	1.13E+01	1.58E+02

*“LB” indicates lower bound, and “UB” indicates upper bound.

References

ACS 2018. U.S. Census Bureau, 2013-2017 American Community Survey 5-Year Estimates. Online: https://factfinder.census.gov/faces/nav/jsf/pages/community_facts.xhtml?src=bkmk. Accessed 9 June 2019.

Alexakhin 1994. R.M. Alexakhin, R.T. Karaban, B.S. Prister, et al., The effects of acute irradiation on a forest biogeocenosis; experimental data, model and practical applications for accidental cases, Science of The Total Environment 157, 357–369 (1994).

Arias 2018. E. Arias and J. Xu, United States Life Tables, 2015, National Vital Statistics Reports 67(7), 64 (2018).

Belgium 2018. Get iodine tablets from the pharmacy | Nuclear Risk; 2018. Online: https://www.nuclearrisk.be/get-iodine-tablets-pharmacy. Accessed 4 June 2019.

Blum 1967. M. Blum and M. Eisenbud, Reduction of Thyroid Irradiation From 131I by Potassium Iodide, JAMA 200(12), 1036–1040 (1967).

Cardis 2005. Cardis, A. Kesminiene, V. Ivanov, et al., Risk of thyroid cancer after exposure to 131I in childhood, J. Natl. Cancer Inst. 97(10), 724–732 (2005).

CFR 2002. Code of Federal Regulation, Title 40, Part 141, Section 141.16 (40 CFR 141.16); 2002. Online: https://www.govinfo.gov/app/details/CFR-2002-title40-vol19/CFR-2002-title40-vol19-sec141-16. Accessed 8 June 2019.

CFR 2019. Code of Federal Regulation, Title 10, Part 20 (10 CFR 20), 2019. Online: https://www.nrc.gov/reading-rm/doc-collections/cfr/part020/index.html. Accessed 8 June 2019.

Conard 1984. R.A. Conard, Late radiation effects in Marshall Islanders exposed to fallout 28 years ago, Radiation carcinogenesis: epidemiology and biological significance (1984).

Davis 2004. S. Davis, K.J. Kopecky, T.E. Hamilton, L. Onstad, and Hanford Thyroid Disease Study Team, Thyroid neoplasia, autoimmune thyroiditis, and hypothyroidism in persons exposed to iodine 131 from the hanford nuclear site, JAMA 292(21), 2600–2613 (2004).

EPA 1995. U.S. Environmental Protection Agency. User’s Guide for the Industrial Source Complex (ISC3) Dispersion Models, Volume II - Description of Model Algorithms. Online: https://www3.epa.gov/scram001/userg/regmod/isc3v2.pdf. Accessed 6 June 2019.

EPA 2017. U.S. Environmental Protection Agency. PAG Manual: Protective Action Guides and Planning Guidance for Radiological Incidents; EPA-400/R-17/001 (2017).

FDA 2001 U.S. Food and Drug Administration. Potassium Iodide as a Thyroid Blocking Agent in Radiation Emergencies. Online: https://www.fda.gov/regulatory-information/search-fda-guidance-documents/potassium-iodide-thyroid-blocking-agent-radiation-emergencies. Accessed 6 June 2019.

FDA 2005. U.S. Food and Drug Administration – CPG Sec. 560.750 Guidance Levels for Radionuclides in Domestic and Imported Foods (CPG 7119.14) Online: https://www.fda.gov/Food/FoodborneIllnessContaminants/ChemicalContaminants/ucm078331.htm. Accessed 6 June 2019.

Gauthier-Lafaye 1996. F. Gauthier-Lafaye, P. Holliger, and P.-L. Blanc, Natural fission reactors in the Franceville basin, Gabon: A review of the conditions and results of a “critical event” in a geologic system, Geochimica et Cosmochimica Acta 60(23), 4831–4852 (1996).

Gifford 1982. F.A. Gifford, Atmospheric Dispersion Models for Environmental Pollution Applications, in Lectures on Air Pollution and Environmental Impact Analyses, edited by D.A. Haugen (American Meteorological Society, Boston, MA, 1982), pp. 35–58.

Google 2017. Google Earth, Imagery Date November 13, 2017. Accessed February 17, 2019.

Higley 2006. K.A. Higley, Environmental consequences of the chernobyl accident and their remediation: twenty years of experience. Report of the chernobyl forum expert group ‘environment,’ Radiation Protection Dosimetry 121(4), 476–477 (2006).

Hosten 2012. 1 B. Hosten, N. Rizzo-Padoin, J.-M. Scherrmann, and V. Bloch, Stable iodine as a prophylaxis therapy following exposure to radioactive iodines: Pharmacological and pharmaceutical characteristics, Annales Pharmaceutiques Francaises 70(2), 75–81 (2012).

Hou 2003. X.L. Hou, C.L. Fogh, J. Kucera, K.G. Andersson, H. Dahlgaard, and S.P. Nielsen, Iodine-129 and Caesium-137 in Chernobyl contaminated soil and their chemical fractionation, Science of The Total Environment 308(1), 97–109 (2003).

IAEA 2015. International Atomic Energy Agency (ed.), The Fukushima Daiichi Accident (International Atomic Energy Agency, Vienna, 2015).

ICRP 1995. International Commission on Radiological Protection. Age-dependent Doses to Members of the Public from Intake of Radionuclides - Part 4 Inhalation Dose Coefficients. ICRP Publication 71. Ann. ICRP 25 (3-4) (1995).

ICRP 2007. International Commission on Radiological Protection. The 2007 Recommendations of the International Commission on Radiological Protection. ICRP Publication 103. Ann. ICRP 37 (2-4) (2007).

ICRP 2012. International Commission on Radiological Protection. Compendium of Dose Coefficients based on ICRP Publication 60. ICRP Publication 119. Ann. ICRP 41(Suppl.) (2012).

ICRP 2015. International Commission on Radiological Protection. Occupational Intakes of Radionuclides: Part 1. ICRP Publication 130. Ann. ICRP 44(2) (2015).

Kerber 1993. R.A. Kerber, J.E. Till, S.L. Simon, et al., A cohort study of thyroid disease in relation to fallout from nuclear weapons testing, JAMA 270(17), 2076–2082 (1993).

Kikuchi 2004. S. Kikuchi, N.D. Perrier, P. Ituarte, A.E. Siperstein, Q.-Y. Duh, and O.H. Clark, Latency Period of Thyroid Neoplasia After Radiation Exposure, Ann Surg 239(4), 536–543 (2004).

Kimura 1987. S. Kimura, T. Kotani, O.W. McBride, et al., Human thyroid peroxidase: complete cDNA and protein sequence, chromosome mapping, and identification of two alternately spliced mRNAs, PNAS 84(16), 5555–5559 (1987).

Knolls Atomic Power Lab 2010. Nuclides and Isotopes : Chart of the Nuclides 17th Edition (Knolls Atomic Power Lab, Schenectady, N.Y., 2010).

Korsakissok 2013. I. Korsakissok, A. Mathieu, and D. Didier, Atmospheric dispersion and ground deposition induced by the Fukushima Nuclear Power Plant accident: A local-scale simulation and sensitivity study, Atmospheric Environment 70, 267–279 (2013).

Lakes 2019. Lakes Environmental. ISCST3 Tech Guide, (n.d.). Online: https://www.weblakes.com/guides/iscst3/section6/6_1_6.html. Accessed 8 June 2019.

Lamarsh 2001. J.R. Lamarsh and A.J. Baratta, Introduction to Nuclear Engineering, 3rd ed (Prentice Hall, Upper Saddle River, N.J, 2001).

Leggett 2017. R. Leggett, An age-specific biokinetic model for iodine, J. Radiol. Prot. 37(4), 864 (2017).

Louisiana Department of Health 2016. Policy Statement. Use of potassium iodide (KI) in Louisiana for emergencies at fixed nuclear facilities; December 2016. (Louisiana DHH Office of Public Health, 325 Loyola Avenue, New Orleans, Louisiana 70160, 2016)

Luxembourg 2014. Preventive distribution of potassium iodide tablets to all residents (21/10/2014) - Home – Infocrise; 2014. Online: https://www.infocrise.lu/en/web/guest/home/-/asset_publisher/uJAlpeXURbmf/content/id/23146. Accessed 4 June 2019.

Mettler 1996. F.H. Mettler, D.V. Becker, B.W. Wachholz, and A.C. Bouville, Chernobyl: 10 years later, J. Nucl. Med. 37(12), 24N, 26N-27N (1996).

MIRD 1975. MIRD Pamphlet No. 11: S, Absorbed Dose per Unit Cumulated Activity for Selected Radionuclides and Organs (1975).

NAACCR 2018. North American Association of Central Cancer Registries, Fast Stats. Online: https://faststats.naaccr.org/selections.php?series=cancer. Accessed 9 June 2019.

National Research Council 2004. National Research Council (ed.), Distribution and administration of potassium iodide in the event of a nuclear incident (National Academies Press, Washington, DC, 2004).

National Research Council 2006. National Research Council (NRC), Health Risks from Exposure to Low Levels of Ionizing Radiation: BEIR VII Phase 2 (National Academies Press, Washington, D.C., 2006).

Nauman 1993. J. Nauman and J. Wolff, Iodide prophylaxis in Poland after the Chernobyl reactor accident: benefits and risks, Am. J. Med. 94(5), 524–532 (1993).

NCI 2019. National Cancer Institute, State Cancer Profiles: Historical Trends. Online: https://statecancerprofiles.cancer.gov/historicaltrend/index.php?0&4322&999&7599&009&080&00&0&0&0&1&0&1&1#results. Accessed 9 June 2019.

Netherlands 2017. Ministerie van Algemene Zaken, Jodiumtabletten - Straling - Rijksoverheid.nl; 2017. Online: https://www.rijksoverheid.nl/onderwerpen/straling/jodiumtabletten. Accessed 4 June 2019.

NOAA 2018. National Oceanic and Atmospheric Administration U.S. Wind Climatology, Societal Impacts | National Centers for Environmental Information. Online: https://www.ncdc.noaa.gov/societal-impacts/wind/w-mean/201805. Accessed 9 June 2019.

NRC 1987. U.S. Nuclear Regulatory Commission. Report on the Accident at the Chernobyl Nuclear Power Station, NUREG-1250 (1987). Online: https://www.nrc.gov/docs/ML0716/ML071690245.pdf. Accessed 9 June 2019.

NRC 2018: U.S. Nuclear Regulatory Commission: River Bend Station, Unit 1; 2018. Online: https://www.nrc.gov/info-finder/reactors/rbs1.html. Accessed 5 June 2019.

Pasquill 1961. F. Pasquill, The Estimation of the Dispersion of Windborne Material, Meteorol. Mag. 90, 33–49 (1961).

Pasquill 1984. F. Pasquill and F. B. Smith. Ellis Horwood, (John Wiley & Sons) Chichester, 1983; Quarterly Journal of the Royal Meteorological Society 110(464), 565–565 (1984).

Prăvălie 2014. R. Prăvălie, Nuclear Weapons Tests and Environmental Consequences: A Global Perspective, Ambio 43(6), 729–744 (2014).

Ruf 2006. J. Ruf and P. Carayon, Structural and functional aspects of thyroid peroxidase, Archives of Biochemistry and Biophysics 445(2), 269–277 (2006).

Shakhtarin 2003. V.V. Shakhtarin, A.F. Tsyb, V.F. Stepanenko, M.Y. Orlov, K.J. Kopecky, and S. Davis, Iodine deficiency, radiation dose, and the risk of thyroid cancer among children and adolescents in the Bryansk region of Russia following the Chernobyl power station accident, Int J Epidemiol 32(4), 584–591 (2003).

Swizterland 2014. Verteilung von Jodtabletten: eine vorsorgliche Schutzmassnahme; 2014. Online: http://www.jodtabletten.ch/. Accessed 4 June 2019.

Till 2008. J.E. Till and H.A. Grogan (eds.), Radiological risk assessment and environmental analysis (Oxford University Press, Oxford ; New York, 2008).

Williams 2003. E.D. Williams, Chernobyl, 15 years later, correlation of clinical, epidemiological and molecular outcomes, Ann. Endocrinol. (Paris) 64(1), 72 (2003).

Zanzonico 2000. P.B. Zanzonico and D.V. Becker, Effects of time of administration and dietary iodine levels on potassium iodide (KI) blockade of thyroid irradiation by 131I from radioactive fallout, Health Phys 78(6), 660–667 (2000).

Vita

Garrett Otis was born and raised in Covington, Louisiana. He enrolled at Louisiana State University (LSU) in 2010 and began an undergraduate teaching role at the university as a supplemental instructor in 2013, which he fulfilled until he received his Bachelor of Science degree in Electrical Engineering in 2015. After working for 2 years as an electrical and instrumentation engineer in the nuclear power industry, he returned to LSU in 2017 to pursue a Master of Science degree from the Medical Physics and Health Physics program. Upon completion of his degree requirements by the end of Summer 2019, he plans to pursue a career in the field of health physics.